J Electr Eng Technol Vol. 8, No. 3: 499-506, 2013
http://dx.doi.org/10.5370/JEET.2013.8.3.499

ISSN(Print) 1975-0102
ISSN(Online) 2093-7423

Algorithm for Fault Location Estimation on Transmission Lines using Second-order Difference of a Positive Sequence Current Phasor

Sang-Min Yeo†, Won-Hyeok Jang* and Chul-Hwan Kim**

Abstract – The accurate estimation of a fault location is desired in distance protection schemes for transmission lines in order to selectively deactivate a faulted line. However, a typical method to estimate a fault location by calculating impedances with voltages and currents at relaying points may have errors due to various factors such as the mutual impedances of lines, fault impedances, or effects of parallel circuits. The proposed algorithm in this paper begins by extracting the fundamental phasor of the positive sequence currents from the three phase currents. The second-order difference of the phasor is then calculated based on the fundamental phasor of positive sequence currents. The traveling times of the waves generated by a fault are derived from the second-order difference of the phasor. Finally, the distance from the relaying point to the fault is estimated using the traveling times. To analyze the performance of the algorithm, a power system with EHV(Extra High Voltage) untransposed double-circuit transmission lines is modeled and simulated under various fault conditions, such as several fault types, fault locations, and fault inception angles. The results of the simulations show that the proposed algorithm has the capability to estimate the fault locations with high speed and accuracy.

Keywords: Fault Location, Traveling wave, Symmetric Sequence, Phasor

1. Introduction

Distance relaying protection schemes for transmission lines require the accurate estimation of a fault location in order to selectively trip a faulted line. Specifically, 756kV double-circuit transmission lines are fundamental facilities in terms of capacity and size, so it is critical to recover from a fault as soon as possible since large amounts of power have to flow on a single line, which increases the risk of another fault. Therefore, a novel algorithm that performs prompt fault detection, identification, and location estimation is needed. The most common algorithm is a method using an impedance calculation which estimates the distance from a fault by calculating the impedance with the voltage and current measured at relaying points. This method, however, is affected significantly by various factors, such as the structure configuration of lines, mutual impedance, and fault impedance. Because of this limitation, an approach with traveling waves has been used since the late 70s. H. W. Dommel and J. M. Michels were the first to present high-speed relaying using traveling wave transient analysis in 1978 [1-11]. Until now, many researchers are studying the traveling wave based fault location algorithm by using various scheme such as wavelet transform, frequency analysis and so on [12-16].

However, existing research with traveling waves has been performed on transposed transmission lines, and algorithms have been developed for single-phase or single-circuit three-phase transmission lines. Traveling waves on single-phase transmission lines are waves that have only one mode, one propagation speed, and one characteristic impedance, while traveling waves on three-phase transmission lines have at least two different propagation speeds and characteristic impedances. Likewise, double-circuit line configurations, such as EHV transmission lines, have six different propagation speeds and characteristic impedances, and these properties are obstacles for fault detection, identification, and location estimation. In addition, EHV transmission lines, which are usually untransposed, have difficulties with distance relay due to the unbalanced impedance of each phase. Therefore, it is necessary to develop an algorithm for fast and accurate fault detection and location estimation for untransposed double-circuit EHV transmission lines.

In order to estimate fault locations even with unbalanced impedance because of multi-circuited and untransposed transmission lines, a novel algorithm using traveling waves, symmetric components, and a phasor is presented in this paper.

2. Traveling Waves Generated by Faults

When a fault occurs on a transmission line, the traveling waves propagate from the fault to both ends of the line. Fig.

† Corresponding Author: Power & Industrial Systems R&D Center, Hyosung Corporation, Korea. (harc@hyosung.com)
* The department of Electrical and Computer Engineering, University of Illinois at Urbana-Champaign, USA. (wjang7@illinois.edu)
** School of Information and Communication Engineering, Sungkyunkwan University, Korea. (hmwkim@hanmail.net)
Received: February 23, 2012; Accepted: January 9, 2013

1 shows the propagation and reflection of traveling waves when there is a forward fault on a transmission line.

Waves are reflected at fault F and both buses A and B. The voltage and current signals are measured at relaying point R. The first backward wave from the fault, f_1, reaches relaying point R at time τ_1 and bus A at time τ. After that, f_1 is reflected at bus A and propagates to the fault F through relaying point R. It is reflected again at fault F and arrives at bus A at time 3τ via relaying point R at τ_3. Also, the first forward wave from the fault, f_3, is reflected at bus B and propagates to the bus A through fault F and relaying point R. τ_5 is the sensing time of the wave f_3 at relaying point R and τ_4 is the arrived time of the wave f_3 at bus A.

Fig. 2 illustrates the propagation of traveling waves for a reverse fault. A relay detects the forward wave, f_2, which travels along the line, passing bus R at time τ_1, rebounds from bus B, and then reaches bus R at time τ_2.

As seen in Figs. 1 and 2, the direction of the initial traveling wave from the forward fault is opposite that from the reverse fault. This simple and clear information can be the criteria used to determine if a forward/reverse fault is within the relay zone. For the forward fault shown in Fig. 1,

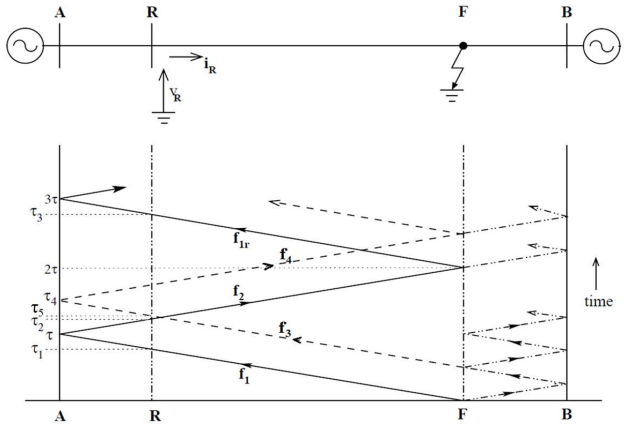

A, B: BUS(or Substation), F: Fault point, R: Relaying point
τ, 2τ, 3τ, τ_4 : arrived time at BUS A τ_1, τ_2, τ_3, τ_5 : sensing time at relaying point

Fig. 1. Propagation and reflection of traveling waves for a forward fault

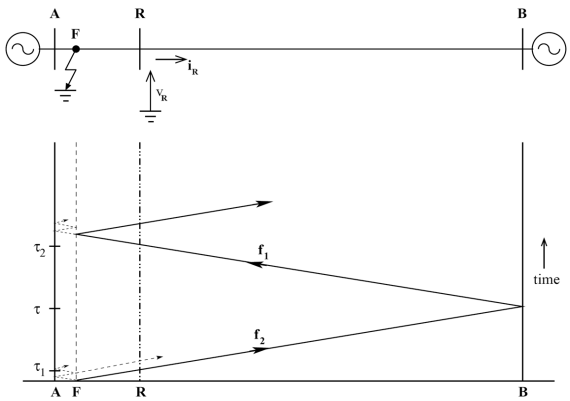

Fig. 2. Propagation of traveling waves for a reverse fault

the fault distance is calculated as the distance between bus A and fault F. Assuming that v is the propagation speed of a traveling wave, the fault distance can be estimated with the propagation speed of a traveling wave and its traveling time from bus A to fault F as

$$d_{F-A} = \frac{v \times (3\tau - \tau)}{2} = \frac{v \times 2\tau}{2} = v \times \tau \tag{1}$$

Since the distance between buses A and R does not change with time, the time difference between the traveling time τ_1 and τ is identical to the difference between τ_3 and 3τ. Also, there is not a transducer such as CT or PT at bus A. Therefore, (1) can be rewritten with the times measured by a relay at bus R as

$$d_{F-A} = \frac{v \times (3\tau - \tau)}{2} = \frac{v \times (\tau_3 - \tau_1)}{2} \tag{2}$$

The first forward wave from the fault in Fig. 1 rebounds from bus B. Part of the wave is reflected at the fault, while the rest of it penetrates through the fault and reaches bus A at time τ_4. Since the line parameters are the same along the transmission line, the propagation speed of the traveling wave between bus A and fault F is identical to that between bus B and fault F. Hence, the distance between fault F and bus B can be calculated with the time difference between τ_1 and τ_4, which are the arrival times of the traveling wave at bus A from fault F and from bus B, respectively. This calculation is presented in (3) and can be rewritten with the time measured at the relaying point R, just as (2) was converted from (1).

$$d_{F-B} = \frac{v \times (\tau_4 - \tau)}{2} \tag{3}$$

Here, note that both the traveling waves at τ and 3τ are the backward wave from the fault in (1) and (2), respectively, whereas the traveling wave measured at τ_4 in (3) is the forward wave from the fault. Also, the fault distance to be ultimately calculated is that between bus A and fault F, which can be estimated by subtracting the distance between bus B and fault F from the whole transmission line length as follows:

$$d_{F-A} = l - d_{F-B} = l - \frac{v \times (\tau_4 - \tau)}{2} \tag{4}$$

3. Algorithm of Fault Location Estimation using Second-Order Difference of Positive Sequence Current Phasor

3.1 Positive sequence phasor

Generally, it is not easy to calculate an unbalanced fault.

Therefore, the method of symmetric coordinates is used to simplify the analysis of unbalanced three-phase systems. This method transforms the unbalanced voltage and current into balanced symmetric components, calculates each component, and then superimposes them again to produce real values [17]. These components are called the positive, negative, and zero sequence components.

In this paper, the positive sequence component, which has the same phase sequence and angle difference as the voltage and current in steady state, is used. The positive sequence component is a vector with properties as follows:

a. Same magnitude for all phases
b. Angle difference of 120°
c. Phase sequence of a-b-c

and can be calculated as

$$I_1 = \frac{1}{3}(I_a + aI_b + a^2 I_c) \tag{5}$$

Here, a is an operator and has the value $a = e^{j120^\circ} = -0.5 + j\sqrt{3}/2$.

A phasor is a representation of a sine wave, such as the voltages and currents in power systems, with information regarding its amplitude and angle. A sine wave signal of a current can be rewritten in complex form as shown in (6).

$$i(t) = I_m \cos(\omega t + \phi) = I_m \,\mathrm{Re}\{e^{j(\omega t+\phi)}\} = I_m \,\mathrm{Re}\{e^{j\omega t} e^{j\phi}\} \tag{6}$$

If the frequency of the current, ω, is fixed, the phasor of the current can be expressed as shown in (7).

$$\mathbf{I} = I_m \angle \phi \tag{7}$$

The phasor representation does not have time information, only amplitude and angle information. Therefore, if the frequency is constant, this representation has an advantage because it simplifies calculations in the analysis of power systems. Among the various methods used to determine the phasor of a voltage or current, the Discrete Fourier Transformation (DFT) is used in this paper. The current in (7) at a sampling rate of N per cycle can be represented with discrete signals as follows:

$$i_k = I_m \cos(\frac{2\pi k}{N} + \phi) \tag{8}$$

The fundamental component extracted from the DFT of (8) is presented in (9) [18].

$$\begin{aligned} I_{fund} &= \frac{2}{N}\sum_{k=0}^{N-1} i_k e^{-j\frac{2\pi}{N}k} \\ &= \frac{2}{N}\sum_{k=0}^{N-1} i_k \cos(-\frac{2\pi}{N}k) + j\frac{2}{N}\sum_{k=0}^{N-1} i_k \sin(-\frac{2\pi}{N}k) \end{aligned} \tag{9}$$

The real and imaginary parts of (9) are I_r and I_i, respectively, and the magnitude and angle of the fundamental wave are I_{mag} and φ, respectively.

$$I_r = \frac{2}{N}\sum_{k=0}^{N-1} i_k \cos(-\frac{2\pi}{N}k) \tag{10}$$

$$I_i = \frac{2}{N}\sum_{k=0}^{N-1} i_k \cos(-\frac{2\pi}{N}k) \tag{11}$$

$$I_{mag} = \sqrt{I_r^2 + I_i^2} \tag{12}$$

$$\phi = \tan^{-1}\frac{I_i}{I_r} \tag{13}$$

The calculated magnitude and the angle of the phasor in (12) and (13) are the current phasor information of the fundamental component, and other components such as harmonics are eliminated. The positive sequence current phasor used in this paper is obtained by inputting the discrete signal for the positive sequence current, I_1, calculated from (5), into (9).

3.2 Second-order difference of positive sequence current phasor

When a fault occurs, the magnitudes of the current and voltage change as the configuration of the power system changes, and the angle difference between the current and voltage also changes depending on the impedance change. The impact of the fault propagates to both ends of the line in the form of traveling waves, as mentioned in Section 3. The voltage and current measured at both ends of the line or relaying points have different magnitudes and forms upon arrival of the traveling waves. Therefore, the direction and the distance of the fault can be estimated by identifying the types of traveling waves and the times of voltage and current change. In this paper, the second-order difference is used in order to determine the arrival times of the traveling waves. The second-order difference can be obtained by calculating the difference between the current sampling value and the previous difference of the first-order difference values. The values of the second-order difference show a sudden large peak when there is a change of voltage or current upon arrival of the traveling waves.

According to the calculation characteristics of the second-order difference, however, the values can differ based on the sampling period. Also, the values are much smaller than the first-order difference, and this could complicate other calculations. Thus, the values have to be scaled for reduced dependence on the sampling period, a simple comparison between the values, and accurate data extraction. In this paper, the reciprocal of 100 times the sampling period is used as the scale factor. The second-order difference equation for the nth sample of the current is presented in (14).

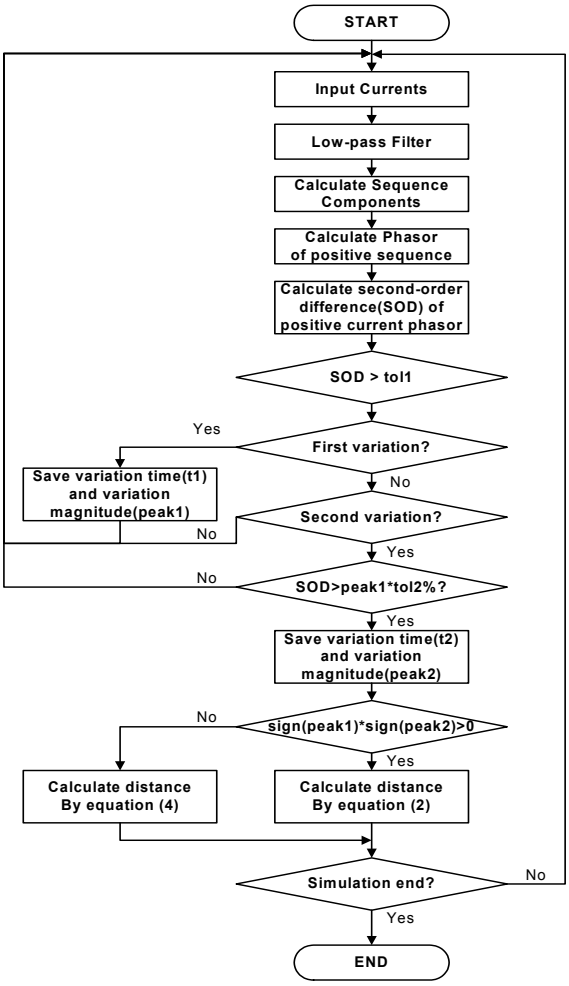

Fig. 3. Algorithm for fault location estimation

$$\begin{aligned} I_{2d,n} &= K \times (I_{1d,n} - I_{1d,n-1}) \\ &= K \times ((I_n - I_{n-1}) - (I_{n-1} - I_{n-2})) \\ &= K \times ((I_n - 2I_{n-1} + I_{n-2})) \end{aligned} \quad (14)$$

where K is the scale factor ($K = 1/([\text{time step}] \times 100)$).

In this paper, the second-order difference for the positive sequence current phasor is calculated using (14) to determine the arrival time of the traveling waves.

3.3 Algorithm for fault location estimation

The proposed algorithm for fault location estimation using the aforementioned second-order difference of the positive sequence current phasor can be organized as follows:

① Input the current value of each phase from relaying points
② Eliminate noise using a low-pass filter (2nd-order butterworth filter, f_{cutoff} =30kHz. In this case, the minimum estimation distance is assumed 5km)
③ Calculate symmetric components for three phase and positive sequence phasors
④ Calculate the second-order difference of positive sequence current phasor
⑤ Compare to determine whether the value at ④ is greater than the criteria, tol1
⑥ Count the peak when it is larger than tol1
⑦ If it is the second peak, compare its value with tol2%
⑧ Compare the first and the second peak values and estimate the fault location

And the flowchart of the proposed algorithm is shown in Fig. 3.

4. Simulations and Results

4.1 Simulation system and conditions

Fig. 4 illustrates the 765kV transmission system used in this study to simulate the algorithm for fault location estimation. It has a three-phase double-circuit transmission line with a length of 137.4km, and a 10^o phase angle difference is applied between the sources to consider the impact of load current. The source impedances are presented in Table 1 [19].

Since EHV transmission lines are not transposed in general, there is an unbalanced impedance between each phase, and this phenomenon affects the existing distance relaying schemes [14]. In order to precisely reflect the characteristics of EHV untransposed transmission lines in the simulation, the transmission line data was calculated with the Line Constants Routine with EMTP. In addition, the line parameters were calculated with the assumption that the transmission lines are untransposed.

Fig. 5 shows the simulation system modeled in EMTP. It has the same structure as the one-line diagram in Fig. 4, and the line data are inputted in frequency-dependent model components.

It is critical to select a proper sampling period to implement the algorithm using traveling waves. If a fault occurs at one end of a transmission line of 100km, the

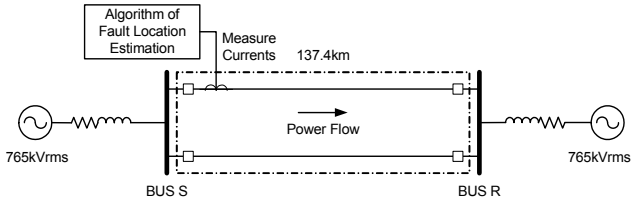

Fig. 4. The 765kV EHV untransposed transmission system

Table 1. Source impedances(unit: ohm)

	Bus S	Bus R
Pos. sequence	0.7607925+j35.9328150	1.5801075+j42.487335
Neg.sequence	0.7607925+j35.7572475	1.5801075+j42.136200
Zero sequence	3.2772600+j39.9708675	6.9056550+j62.560553

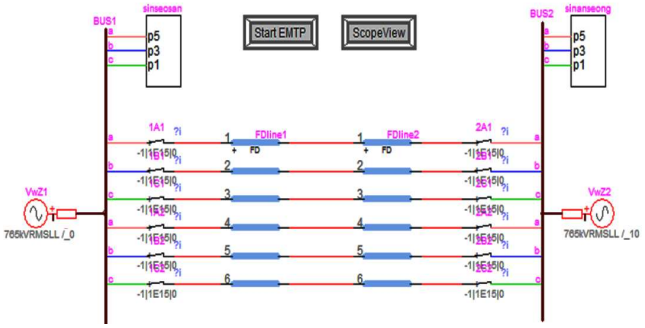

Fig. 5. Simulation system modeled with EMTP

Table 2. Fault conditions

Fault type	single line-to-ground, double line-to-ground, line-to-line, and three-phase fault
Fault angle	0^o, 45^o, 90^o
Fault distance	13.74km~123.66km (every 10% of the total line length)

propagation time of a traveling wave to the other end and back to the fault is t=200[km]/(3x10^6[km/s])=1.5x10^{-3}[s]. Likewise, the time for a fault at 1km is t=1.5x10^{-3}[s]. Without counting the waves generated at the other end, the traveling waves arrive at the origin at least once every 15us. In other words, the sampling period has to be a minimum of 15us to make the algorithm accurate within 1km. Therefore, the sampling period has to be short enough to precisely implement the algorithm. Generally, relay algorithms using traveling waves have a high sampling frequency. In this paper, 32768 sampling times were conducted for the fundamental frequency of 60Hz. The simulation time chosen considering the sampling rate was 0.5us. All of the possible fault conditions on a transmission line were considered in the simulations to evaluate the proposed algorithm, as shown in Table 2.

4.2 Simulation results

Fig. 6 depicts the fault current waveform for a single line-to-ground fault with a 0Ω fault resistance and a 90^o fault angle occurring at 20% of the line length, which is 27.48km of Circuit 1 in the double-circuit transmission system. Harmonics were observed in the waveform due to the fault. The positive sequence current phasor can be calculated from the fault current in Fig. 6, and its magnitude is presented in Fig. 7.

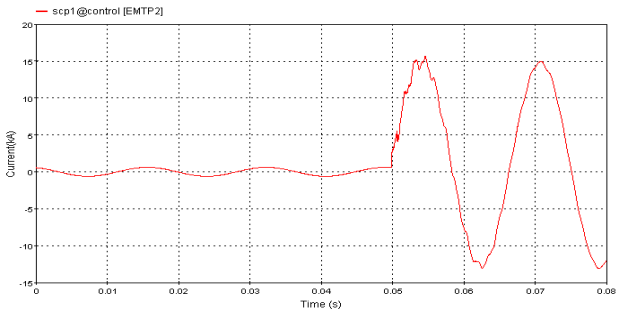

Fig. 6. Waveform of instantaneous current at faulted phase

As mentioned previously, it is difficult to determine the magnitude change due to the arrival of traveling waves using only the magnitude of the positive sequence current phasor, as in Fig. 7. Fig. 8 shows the waveform of the second-order difference of the positive sequence current phasor with a lower bound after filtering.

A considerable peak value appears in Fig. 8 when there is a change in the positive sequence current phasor. Fig. 9 shows the magnified graph at the time of the fault in Fig. 8. Peaks appear periodically due to the traveling waves generated after the fault, and the fault distance can be estimated using these peak times.

In this case, the information about the first and second peaks is as follows:

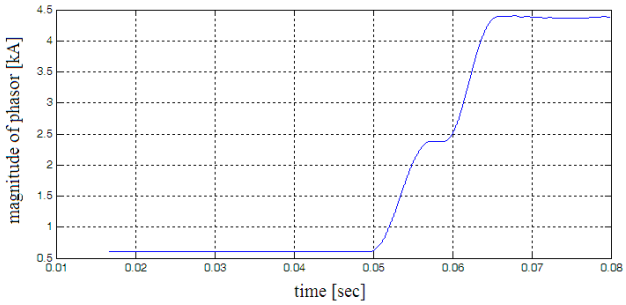

Fig. 7. Magnitude of positive sequence current phasor

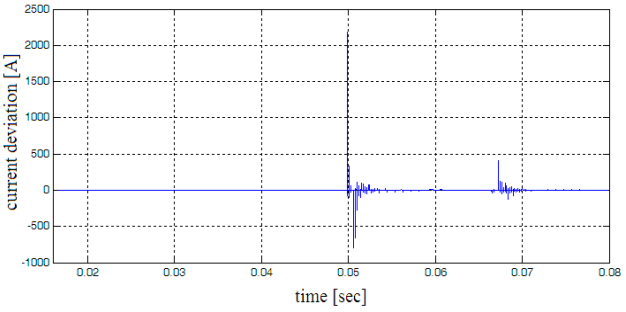

Fig. 8. Second-order difference of the positive sequence current phasor

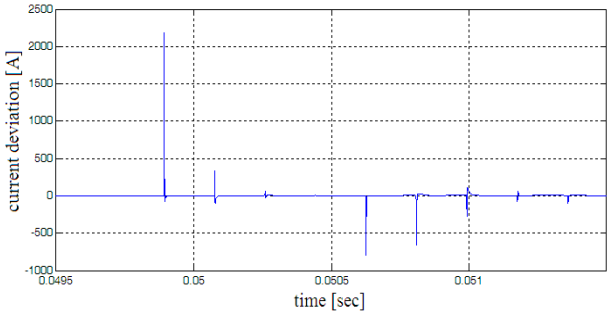

Fig. 9. Enlargement of Fig. 8 after a fault

Table 3. Results for all simulation conditions

Fault type			Fault distance								
			10% (13.74km)	20% (27.48km)	30% (41.22km)	40% (54.96km)	50% (68.7km)	60% (82.44km)	70% (96.18km)	80% (109.92km)	90% (123.66km)
Single line-to-ground	0°	Estimated distance	13.651	27.460	41.193	54.926	68.659	82.392	96.125	109.934	123.667
		Error rate	0.06%	0.01%	0.02%	0.02%	0.03%	0.03%	0.04%	0.01%	0.01%
	45°	Estimated distance	13.651	27.542	41.351	55.084	68.659	82.392	96.201	109.934	123.667
		Error rate	0.06%	0.05%	0.10%	0.09%	0.03%	0.03%	0.02%	0.01%	0.01%
	90°	Estimated distance	13.651	27.542	41.351	55.084	68.659	82.392	96.125	109.934	123.667
		Error rate	0.06%	0.05%	0.10%	0.09%	0.03%	0.03%	0.04%	0.01%	0.01%
Double line-to-ground	0°	Estimated distance	13.651	27.384	41.193	54.926	68.659	82.468	96.201	109.934	123.667
		Error rate	0.06%	0.07%	0.02%	0.02%	0.03%	0.02%	0.02%	0.01%	0.01%
	45°	Estimated distance	13.651	27.384	41.193	54.926	68.659	82.468	96.201	109.934	123.667
		Error rate	0.06%	0.07%	0.02%	0.02%	0.03%	0.02%	0.02%	0.01%	0.01%
	90°	Estimated distance	13.651	27.384	41.117	54.926	68.659	82.392	96.201	109.934	123.591
		Error rate	0.06%	0.07%	0.07%	0.02%	0.03%	0.03%	0.02%	0.01%	0.05%
Line-to-line	0°	Estimated distance	13.651	27.460	41.193	54.926	68.659	82.468	96.201	109.934	123.667
		Error rate	0.06%	0.01%	0.02%	0.02%	0.03%	0.02%	0.02%	0.01%	0.01%
	45°	Estimated distance	13.651	27.384	41.193	54.926	68.659	82.468	96.201	109.934	123.667
		Error rate	0.06%	0.07%	0.02%	0.02%	0.03%	0.02%	0.02%	0.01%	0.01%
	90°	Estimated distance	13.651	27.384	41.117	54.926	68.659	82.392	96.201	109.934	123.667
		Error rate	0.06%	0.07%	0.07%	0.02%	0.03%	0.03%	0.02%	0.01%	0.01%
Three-phase	0°	Estimated distance	13.651	27.384	41.193	54.926	68.659	82.468	96.201	109.934	123.667
		Error rate	0.06%	0.07%	0.02%	0.02%	0.03%	0.02%	0.02%	0.01%	0.01%
	45°	Estimated distance	13.651	27.384	41.193	54.926	68.659	82.468	96.201	109.934	123.667
		Estimated distance	0.06%	0.07%	0.02%	0.02%	0.03%	0.02%	0.02%	0.01%	0.01%
	90°	Estimated distance	13.651	27.384	41.117	54.926	68.659	82.392	96.201	109.934	123.591
		Error rate	0.06%	0.07%	0.07%	0.02%	0.03%	0.03%	0.02%	0.01%	0.05%

- t1 = 0.049892141592 sec, peak1 = 1531.269318 A
- t2 = 0.050075755578 sec, peak2 = 337.87493 A

Since the signs of the two peaks are identical, the fault distance can be calculated as shown in (15), according to (2). The propagation speed is assumed to be the speed of light, $3.0\text{x}10^5$km/s.

$$\begin{aligned} d &= \frac{v \times (\tau_3 - \tau_1)}{2} \\ &= 3.0 \times 10^5 \times (0.0500757558 - 0.04989214192)/2 \\ &= 3.0 \times 10^5 \times (0.000183613986)/2 = 27.542098[\text{km}] \end{aligned} \quad (15)$$

The real fault distance is 27.48km, and the error rate of the estimated distance can be calculated as shown in (16).

$$\begin{aligned} \text{error rate} &= \frac{\left|(\text{real value}) - (\text{estimated value})\right|}{(\text{total length})} \times 100[\%] \\ &= \frac{\left|27.48 - 27.54\right|}{137.4} \times 100 = \frac{0.06}{137.4} \times 100 \\ &= 0.045[\%] \end{aligned} \quad (16)$$

All of the results for the simulation conditions in Table 2 are presented in Table 3. The error rates are calculated with respect to each fault type, fault angle, and fault distance.

The simulation results verify that the proposed algorithm produces a very accurate estimation of the fault location. The largest error rate is 0.1% for the two simulation conditions: a single line-to-ground fault with a 45° fault angle at 30% distance, and a single line-to-ground fault with a 90° fault angle at 30% distance. However, a 0.1% error rate is negligible since it represents only 0.13km, indicating that the performance of the algorithm is outstanding.

5. Conclusions

In this study, an algorithm for fault location estimation using the second-order difference of a positive sequence current phasor was proposed. The performance of the algorithm was evaluated with respect to various simulation conditions of fault type, fault distance, and fault angle. The simulation results in Table 3 show that the algorithm has a very small error rate less than 0.1%.

Typically, algorithms with traveling waves demand very fast sampling and large memory capacity, and this causes various physical constraints for their actual development. However, the proposed algorithm uses less data than existing algorithms, which require both voltage and current. Using only the second-order difference of the positive sequence current phasor and simple equations, this algorithm is more feasible and efficient to implement compared to existing methods. For future work, the non-fault cases will be considered.

References

[1] M. M. Mansour, G. W. Swift, "A multi-microprocessor based travelling wave relay-theory and realization," IEEE Transactions on Power Delivery, Vol. 1, No. 1, pp. 272-279, Jan. 1986.

[2] S. Wajendra, P. G. McLaren, "Traveling-wave techniques applied to the protection of teed circuits: principle of traveling wave techniques," IEEE Transactions on Power Apparatus and Systems, Vol. PAS-104, No. 12, pp. 3544-3550, Dec. 1985.

[3] S. Rajendra, P. G. McLaren, "Traveling wave techniques applied to the protection of teed circuits: Multi-phase/multi circuit system," IEEE Transactions on Power Apparatus and Systems, Vol. PAS-104, No. 12, pp. 3551-3557, Dec. 1985.

[4] E. H. Shehab-Eldin, P. G. McLaren, "Traveling wave distance protection- problem areas and solutions," IEEE Transactions on Power Delivery, Vol. 3, No. 3, pp. 894-902, July 1988.

[5] J. Blake, P. Tantaswadi, R. T. de Carvalho, "In-line Sagnac interferometer current sensor," IEEE Transactions on Power Delivery, Vol. 11, No. 11, pp. 116-121, Jan. 1996.

[6] F. H. Magnago, A. Abur, "Fault location using wavelets," IEEE Transactions on Power Delivery, Vol. 13, No. 4, pp. 1475-1480, Oct. 1998.

[7] M. Silva, M. Oleskovicz, D. V. Coury, "A fault locator for transmission lines using traveling waves and wavelet transform theory," Eighth IEE International Conference on Developments in Power System Protection, Vol. 1, pp. 212-215, 5-8 April 2004.

[8] A. Elhaffar, M. Lehtonen, "Travelling waves based earth fault location in 400 kV transmission network using single end measurement," Large Engineering systems Conference on Power Engineering, pp. 53-56, July 2004.

[9] W. Dai, M. Fang, L. Cui, "Traveling wave fault location system," World Congress on Intelligent Control and Automation, Vol. 2, pp. 7449-7452, June 2006.

[10] N. Perera, A. D. Rajapakse, A. M Gole, "Wavelet-based relay agent for isolating faulty sections in distribution grids with distributed generators," The 8th IEE International Conference on AC and DC Power Transmission, Vol. 513, pp. 162-166, Mar. 2006.

[11] H. W. Dommel, J. M. Michels, "High speed relaying using traveling wave transient analysis," IEEE PES Winter Power Meeting, New York, No. 78 CH1295-5 PWR, paper No. A78 214-9, pp. 1-7, Jan. 1978.

[12] Y. J. Kwon, S. H. Kang, D. G. Lee, H. K. Kim, "Fault location algorithm based on cross correlation method for HVDC cable lines," IET 9th International Conference on Developments in Power System Protection 2008, pp. 360-364, 17-20 Mar. 2008.

[13] Jiantao Sun, Xishan Wen, Xinlao Wei, Qingguo Chen, Yonghong Wang, "Traveling Wave Fault Location for Power Cables Based on Wavelet Transform", 2007 International Conference on Mechatronics and Automation, pp.1283-1287, 5-8 Aug. 2007.

[14] S. Lin, Z.Y. He, X.P. Li,Q.Q. Qian, "Travelling wave time-frequency characteristic-based fault location method for transmission lines", IET Generation, Transmission & Distribution, Vol. 6, No. 8, pp.764-772, August 2012.

[15] V. Kale, S. Bhide, P. Bedekar, "Fault Location Estimation Based on Wavelet Analysis of Traveling Waves", Asia-Pacific Power and Energy Engineering Conference (APPEEC) 2012, pp.1-5, 27-29 March 2012.

[16] L.U. Iurinic, A.S. Bretas, E.S. Guimaraes, D.P. Marzec, "Analysis of single-ended traveling-wave fault location based on continuous wavelet transform inferred from signal", 11th International Conference on DPSP 2012, pp. 1-6, 23-26 April 2012.

[17] P. M. Anderson, "Analysis of faulted power systems," IEEE PRESS Power Systems Engineering Series, 1995.

[18] A. G. Phadke, J. S. Thorp, M. G. Adamiak, "A new measurement technique for tracking voltage phasors, local system frequency, and rate of change of frequency," IEEE Transactions on Power Apparatus and Systems, Vol. PAS-102, No. 5, pp. 1025-1038, May 1983.

[19] Y. J. Ahn, S. H. Kang, "A study on the transient characteristics in 765kV untransposed transmission systems," Transactions on KIEE, Vol. 53A, No. 7, pp. 397-404, July 2004.

Sang-Min Yeo He received his B.S., M.S., and Ph.D. degrees in Electrical Engineering from Sungkyunkwan University in 1999, 2001, and 2009, respectively. Since October 2009, he joined Power & Indus-trial Systems R&D Center, Hyosung Corporation, Korea. His current research interests include power system transients, modeling and simulation for FACTS/ HVDC using EMTP, power system protection and computer application using EMTP, and signal processing.

Won-Hyeok Jang He received his B.S. and M.S. in Electrical and Computer Engineering from Sungkyunkwan University, Suwon, Korea in 2008 and 2010, respectively. He is now working toward his Ph.D. degree at University of Illinois at Urbana-Champaign. He is a Research Assistant in Electrical and Computer Engineering Department, University of Illinois at Urbana-Champaign. His research interests include power system modeling and analysis.

Chul-Hwan Kim He received his B.S., M.S., and Ph.D degrees in Electrical Engineering from Sungkyunkwan University, Korea, 1982, 1984, and 1990 respectively. In 1990 he joined Cheju National University, Cheju, Korea, as a full-time Lecturer. He has been a visiting academic at the University of BATH, UK, in 1996, 1998, and 1999. Since March 1992, he has been a professor in the School of Information and Communication Engineering, Sungkyunkwan University, Korea. His research interests include power system protection, artificial intelligence application for protection and control, the modeling/protection of underground cable and EMTP software.